

# Inverse Design Method of Wide Range Self-starting Inward-turning Inlet Based on the Concept of Double Design Points

Zejun Cai<sup>1</sup>, Xiaogang Zheng<sup>1</sup>, Menglei Guo<sup>1</sup>, Zhenqi Sun<sup>1</sup>, Chengxiang Zhu<sup>1</sup>, Yancheng You<sup>1</sup>

## **Abstract**

Hypersonic vehicles require higher inlet performance across expanding flight envelopes. Inward-turning inlets offer high compression efficiency and mass capture but suffer from low-Mach starting difficulty due to that efficiency. Conventional single-point designs struggle with wide-speed-range performance. To address this, this paper proposes a wide-speed-range self-starting internal contraction inlet inverse design method based on the Double Design Points (DDP) concept. The method constructs a DDP self-starting basic flow field by controlling internal/external compression strengths and generates the 3D inlet surface via the osculating method to inherit the flow field characteristics. Numerical simulations confirm full mass flow capture at the high Mach number design point (Ma6) and self-starting capability at the low Mach number design point (Ma4.5). During starting, the large separation bubble causing unstart is gradually engulfed by the throat, shrinking into a small bubble. This provides a new approach to enhance inlet wide-speed-range capability.

## 1. Introduction

Hypersonic inlets are critical components of air-breathing propulsion systems, responsible for delivering high-quality airflow to the engine<sup>1,2</sup>. The primary configurations include axisymmetric inlets, two-dimensional inlets, and inward-turning inlets. Among these, inward-turning inlets have gained significant research attention in recent years. This configuration has been embraced by several developments in hypersonic aircraft, including the SR-72 <sup>3</sup>, HAWC <sup>4</sup>, and Boeing's hypersonic aircraft <sup>5</sup> Inward-turning inlets offer advantages including reduced windward area, superior mass flow capture capability, and efficient flow compression<sup>1</sup>. However, they also exhibit inherent limitations such as poor low-Mach number starting characteristics and design complexity associated with three-dimensional curvature.

To tackle this, researchers proposed lots of studies about the starting capability of the inlet. The analysis of starting capability is typically based on the Kantrowitz limit <sup>6</sup> and the isentropic limit. They are proposed based on the one-dimensional quasi-steady flow theory. The isentropic limit describes the flow tube passage capability under fully isentropic compression. The Kantrowitz limit describes it considering normal shock losses. Van extended these to the inlets' starting analysis, using the internal contraction section Mach number and internal contraction ratio to assess starting status <sup>7</sup>. The isentropic limit analyzes starting capability – whether an inlet becomes unstarted due to over-compression at the current inflow condition. The KW limit analyzes self-starting capability – the ability to spontaneously restart after unstarted when the unstarted trigger ceases. Van Wie's research shows the KW limit is conservative: inlets can self-starting at a status lower than the KW limit <sup>8</sup>. Consequently, Sun fitted a self-starting boundary from wind tunnel test data on inward-turning inlets, proposing a more reliable boundary <sup>9</sup>.

These theories are widely applied in starting capability analysis, but not in aerodynamic design. Therefore, to construct an inward-turning inlet with wide speed range operability, this paper develops an inverse design method for controllable wide speed range self-starting based on the concept of Double Design Points (DDP) <sup>10</sup>. By selecting an additional low-Mach design condition based on self-starting requirements, it controls the internal contraction Mach number (Ma-inner) at this point while applying the self-starting limit. This approach achieves controllable inlet self-starting capability through the coordinated design of internal/external contraction ratios.

HiSST-2024-xxxx Paper Title

<sup>&</sup>lt;sup>1</sup> Xiamen University, Xiamen Fujian, caizejun@stu.xmu.edu.cn

# 2. Self-starting inward-turning inlet design method

## 2.1. Relationships between design parameters and self-starting capability

To achieve controllable self-starting capability over a wide operating range, this study develops a design method for inward-turning inlets with wide-range self-starting characteristics based on the Double Design Point (DDP) concept proposed earlier. This approach incorporates self-starting analysis within the low Mach number design point to ensure controllable self-starting characteristics across the design envelope.

The first step involves analyzing how inlet starting and self-starting capabilities correlate with various aerodynamic and design parameters. Hypersonic inlets essentially function as flow tubes for capturing and compressing high-speed airflow. Researchers have developed one-dimensional starting capability analysis methods based on continuity, energy, and momentum equations, known as the Isentropic criterion and the Kantrowitz criterion. Fig. 1 presents the starting boundaries plotted according to these criteria, with the Mach number at the internal compression section on the abscissa and the inverse of the internal contraction ratio (ICR) on the ordinate. The diagram is divided into three regions: areas to the left of the Isentropic boundary represent the unstart state, while regions to the right of the Kantrowitz criterion indicate inlets with self-starting capability. The central region represents the dual-solution zone, where the starting capability depends on the initial state of flow field. However, experimental and numerical simulations reveal that actual self-starting boundaries often fall below the Kantrowitz criterion, suggesting that inlets can achieve self-starting at higher ICR than predicted. Sun et al. proposed an empirical self-starting boundary (the blue curve in Fig. 1) based on existing data.

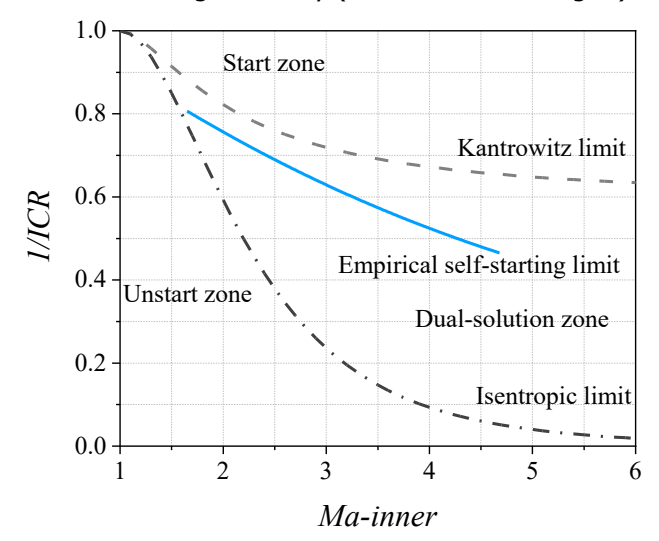


Fig. 1 Deconstruction of double design point basic flow field

This fitted self-starting boundary provides a more accurate criterion for analysing inlet self-starting capability. However, relying solely on this criterion cannot promptly and effectively support inlet design, as it requires numerical methods to determine the Mach number at the internal contraction section after completing the design scheme. Consequently, evaluating the self-starting capability under specified conditions necessitates extensive iterative optimization processes.

## 2.2. Design process of self-starting basic flow field

To incorporate wide-range self-starting capability into the inlet design process, this paper proposes a basic flowfield inverse design method with controllable wide-range self-starting capability by integrating the previously established double design points method with the aforementioned self-starting criterion.

As illustrated in Fig. 2, the basic flowfield consists of three regions: the shock-determination region (Region ①), the low Mach number mass flow rate control region (Region ②), and the self-starting capability design region (Region ③). Region ① defines the incident shock shape for both high and low Mach number design points. To achieve full mass flow capture at the high Mach number design point, the lip point is positioned on the high Mach number incident shock, and its location is determined by

the given centerbody height. At the low Mach number design point, the required flow tube height for capture in Region ① is calculated using Equation (1), yielding a streamline as the lower boundary of the flow tube. This streamline, termed the lip streamline, extends downstream to the lip point in Region ②, ensuring the intended mass flow capture capability. In Region ③, the design must satisfy two conditions: the reflected shock intersects the upper wall at the shoulder in the high Mach number flowfield, and the intersection point maintains a specified height to meet the total contraction ratio requirement.

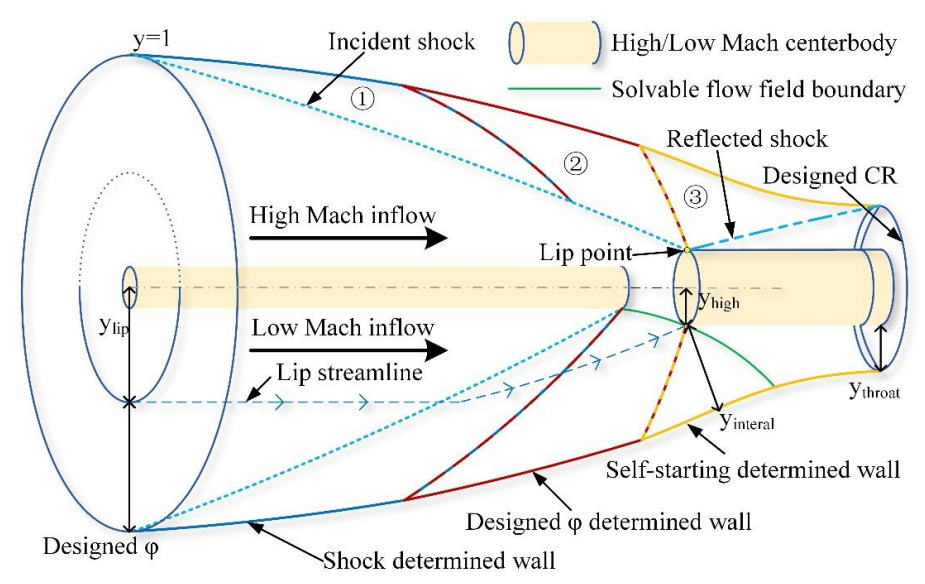


Fig. 2 Deconstruction of double design point basic flow field

$$\varphi = \frac{y_{begin}^2 - y_{lip}^2}{y_{begin}^2 - h_{high}^2} \tag{1}$$

The design procedure of the self-starting DDP basic flow field is shown in Fig. 4. At the beginning, the wall boundary I is constructed according to the given high Mach number design point incident shock, and the corresponding high/low Mach flow field 1 is calculated. After that, the design process goes to construct wall boundary II and III. The low Mach mass flow rate is an important prediction and correction parameter in the remaining process.

Firstly, a lip streamline is generated in the low Mach flow field 1 according to the initial low Mach mass flow rate, which would be changed to match the target contraction ratio (TCR). Then, the wall boundary II is generated through a simplified DDP process, and the corresponding low Mach flow field 2 would lead the lip streamline to the lip point. The external contraction ratio (ECR) and internal Mach number (Maint) are calculated for the remaining design process and self-starting control. Through the self-starting analysis (in Fig. 1), the startable internal contraction ratio (ICR) is proposed. And the wall boundary III is created according to the ICR. Then, the current contraction ratio (CCR) is compared with TCR, and the mass flow rate is rearranged, and the process goes to design the wall boundaries II and III again, until the discrepancy between CCR and TCR is acceptable

Fig. 4 illustrates the core process of the self-starting control. The self-starting procedure employs a simplified DDP method. Traditional DDP methods use a step forward wall design process. This step forward process provides a larger design space and higher precision for the mass flow rate control. In contrast, the present method utilizes the DDP approach solely to simultaneously control the Ma-inner and ECR. Consequently, the shapes of Wall II and Wall III are defined using Bézier curves. This definition simplifies the design steps and reduces computational effort. Within the simplified DDP method, the coordinates of the Bézier curve control points are adjusted. This adjustment allows Wall II to maintain curvature continuity with Wall I. Simultaneously, the curve shape changes to match the specified mass flow rate. Building upon this simplified DDP method, Flow Field ② uses the mass flow rate as the control input. This input alters the ECR and Ma-inner. The self-starting internal contraction ratio is then determined based on the starting criterion. The corresponding current contraction ratio

(CCR) is also identified. The difference between CCR and TCR serves as the criterion. The flow coefficient is modified to ensure this difference meets the specified error tolerance.

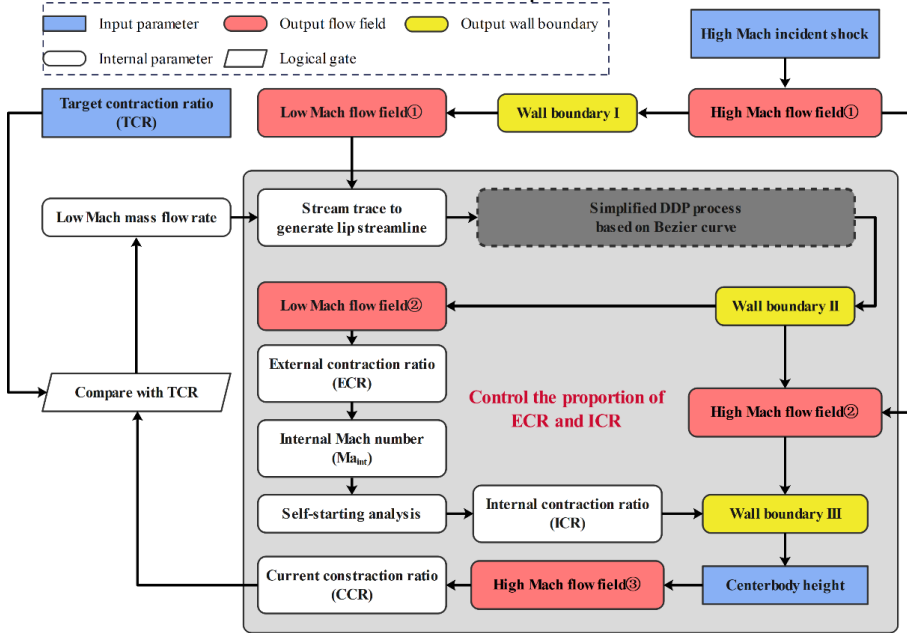


Fig. 3 Design procedure of self-starting DDP basic flow field

Fig. 4 illustrates the design principle and process of constructing Wall II using a simplified DDP method. The conventional DDP method typically employs a step-forward design to enhance the designability and accuracy of  $\phi$ , at a cost of low computational efficiency. Since the primary objective of the self-starting capability is to control the external compression intensity of the basic flow field through  $\phi$ , accuracy is secondary. Consequently, the wall definition is simplified to improve computational efficiency. Wall II is defined by a Bézier curve, whose control points govern the lip streamline shape and thus match the  $\phi$ .

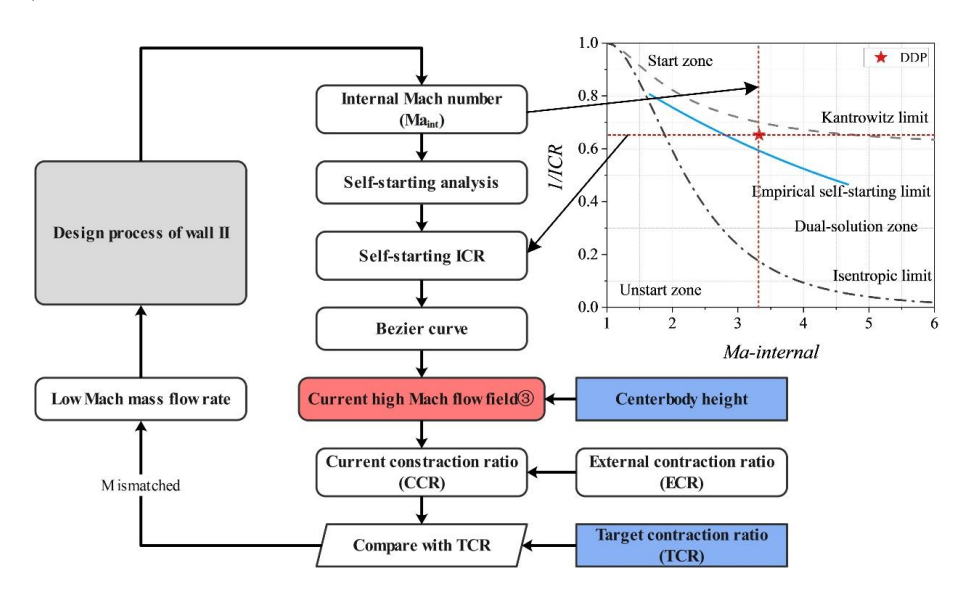


Fig. 4 Self-starting control method in wall II design process

## 2.3. Osculating self-starting inward-turning inlet design process

Streamline tracing is a common method for generating inlet surfaces in inward-turning inlet design. It involves extracting a flow tube with a specified entry shape from a basic flow field. Deviations in aerodynamic performance, particularly in parameters critical to self-starting capability like internal contraction Mach number and internal contraction ratio, occur between the inlet and the basic flow field depending on the extracted flow tube shape. Consequently, streamline tracing solely within the self-starting basic flow field designed in this work cannot guarantee identical starting capability. While

employing a fan-shaped entry shape achieves aerodynamic performance identical to the basic flow field, it severely restricts design freedom. To address this, this paper implements free-form entry shape design and controllable three-dimensional internal contraction ratio design using the osculating method and child basic flow field design. The design principle is illustrated in Fig. 5.

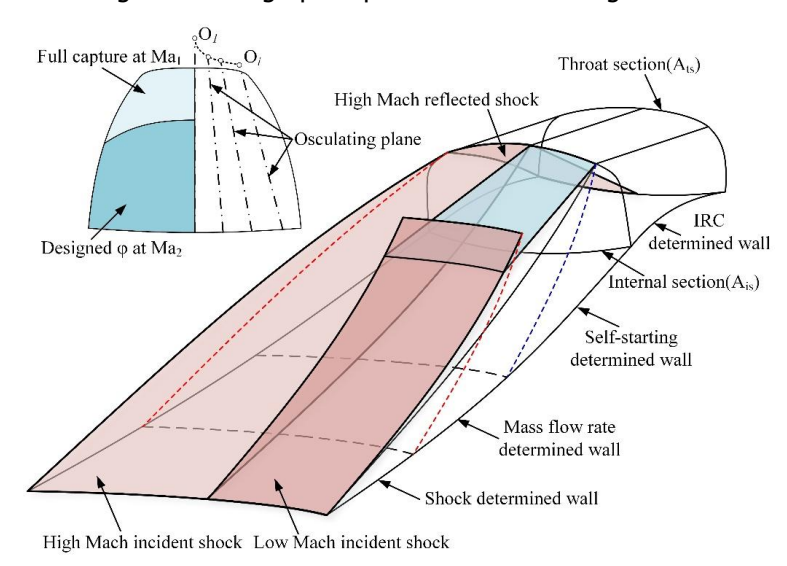


Fig. 5 Design procedure of osculating self-starting inward-turning inlet

Within a given entry shape, the leading edge profile is discretized into a series of points. These points and their curvature centers establish a local coordinate system within the osculating plane, where the origin is the curvature center. The aerodynamic profile of the inlet results from assembling the wall generatrices of local basic flow fields within each osculating plane. The osculating plane with the largest curvature radius contains the parent basic flow field, designed using the DDP self-starting basic flow field. Flow fields in other osculating planes, termed child basic flow fields, derive from the parent flow field. Fig. 6 illustrates the method for designing the child basic flow field based on the parent basic flow field. The child flowfield design also comprises three parts. Wall I, the incident shock-determined segment, is obtained by streamline tracing within the parent flowfield. This approach could make the flow reside within the osculating plane better, other than being affected by the pressure gradient between osculating planes. Consequently, enhance the effectiveness of subsequent design. Walls II and III are then constructed using the simplified DDP method.

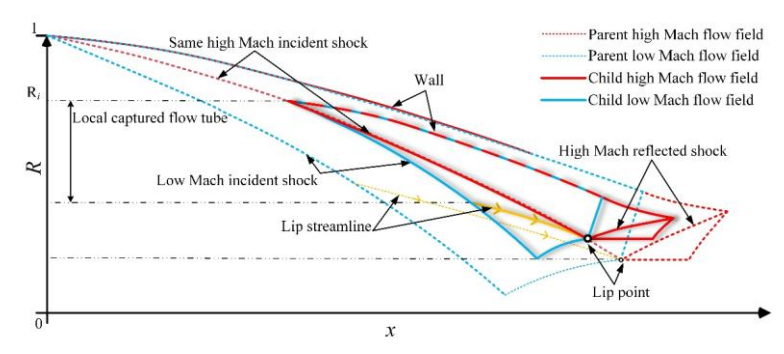


Fig. 6 Design method of child DDP self-starting basic flow field

# 3. Numerical verification and analysis

# 3.1. Numerical methods

The numerical method described in the previous section was employed in this study to simulate the experimental model presented in [31]. The cross-section of the model is shown in Fig. 7 (a), and the inflow conditions are based on the reference in [31]. Fig. 7(b) compares the pressure distribution on the upper and lower walls between the experiment and simulation. It can be observed that both the numerical and experimental results exhibit close agreement in terms of the pressure distribution and

overall trend. The above validation demonstrates the accuracy of the computational method used in this study, supporting the simulation-based investigation of the aerodynamic performance presented in this paper.

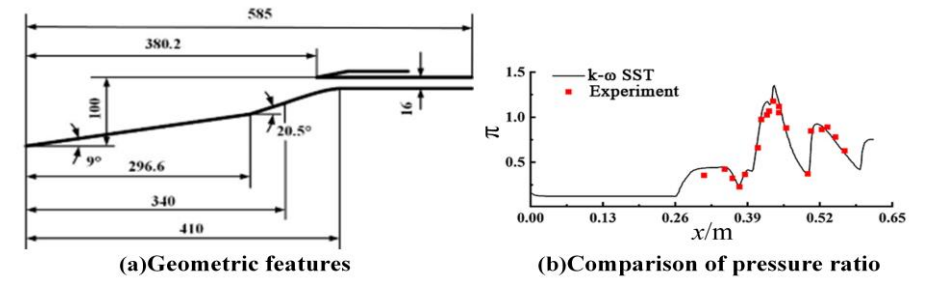


Fig. 7 Numerical example verification of cases and comparison of wall pressure distribution

The present study solves the three-dimensional Reynolds-Averaged Navier-Stokes (RANS) equations based on density. The inviscid convective fluxes are computed using the second-order upwind Roe-FDS differencing scheme. The convergence criterion for the computational process is to reduce the residuals of the continuity equation, momentum equation, and energy equation by at least three orders of magnitude, while ensuring a stable mass flow rate at the outlet cross-section of the inlet duct. Air is assumed to be an ideal gas, with the specific heat capacity at constant pressure (Cp) modeled using a Piecewise-Polynomial fit. As shown in Fig. 8(a), the freestream face is defined as the pressure far-field boundary, while the outlets are considered pressure outlets. The wall boundaries are treated as adiabatic with no-slip conditions, neglecting heat transfer. To meet the scale requirements of different design point Mach numbers, multiple sets of computational grids are employed in this study. Each grid set is refined near the wall surface, ensuring a y+ value of no greater than 30. In order to accommodate the diverse flow conditions associated with different Mach numbers, several computational grid configurations are utilized.

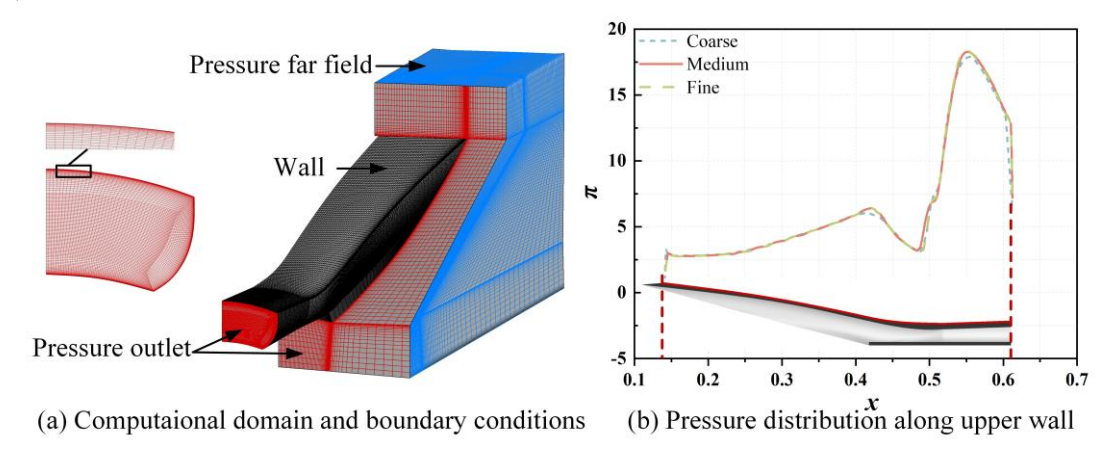
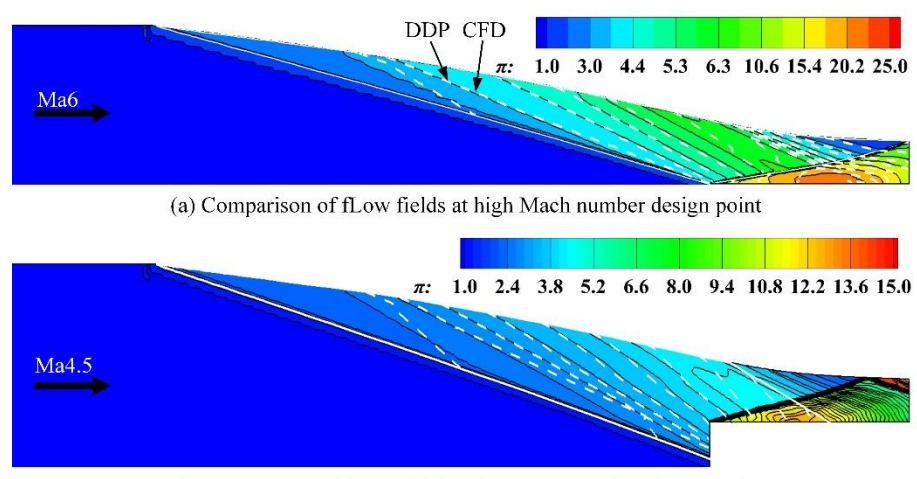


Fig. 8 The CFD calculation settings and grid sensitivity analysis

To ensure the reliability of the computational results, a grid independence verification was conducted. This involved a comparison of coarse, medium, and fine grids, as depicted in Fig. 8(b). It portrays the pressure ratio along the intersection line between the upper wall and the symmetry plane. The vertical axis represents the pressure ratio of wall curve at symmetry plane, while the horizontal axis corresponds to the x-direction coordinate. Notably, the pressure ratio demonstrates a consistent trend across various mesh sizes, with all curves fitting well. Consequently, this article adopts a medium grid size for the numerical simulation. The grid resolution for other computational conditions was adjusted accordingly.

## 3.2. Self-starting basic flow field verification

To validate the effectiveness of the double design point (DDP) basic flowfield design method, twodimensional inviscid numerical simulations were conducted. Fig. 9 compares the numerical results with the DDP flowfield, where white dashed lines represent pressure contours obtained from DDP, and colored contours with solid black lines depict the CFD-calculated flowfield. At the high Mach number design point, the incident shock intersects the lip point, and the reflected shock meets the upper wall at the shoulder, forming a two-shock three-region structure. The good agreement between DDP and CFD contours demonstrates the validity of the design method under this condition. Similarly, at the low Mach number design point, both the incident shock and contour distributions show close correspondence, further confirming the method's accuracy across different operating conditions.



(b) Comparison of fLow fields at low Mach number design point

Fig. 9 Verification of double design point method

Furthermore, to validate the self-starting capability, the exit conditions were modified to induce an unstarted flow, followed by restoring normal flow-through conditions. As shown in Fig. 10, in the unstarted state, the incident shock is replaced by a normal shock positioned upstream, and the internal contraction section becomes a subsonic region, losing its usual flow capture capability. Upon restoring the exit conditions, the incident shock begins propagating downstream, the subsonic region exits through the outlet, and supersonic flow is re-established in the internal contraction section. The basic flowfield successfully demonstrates self-starting capability.

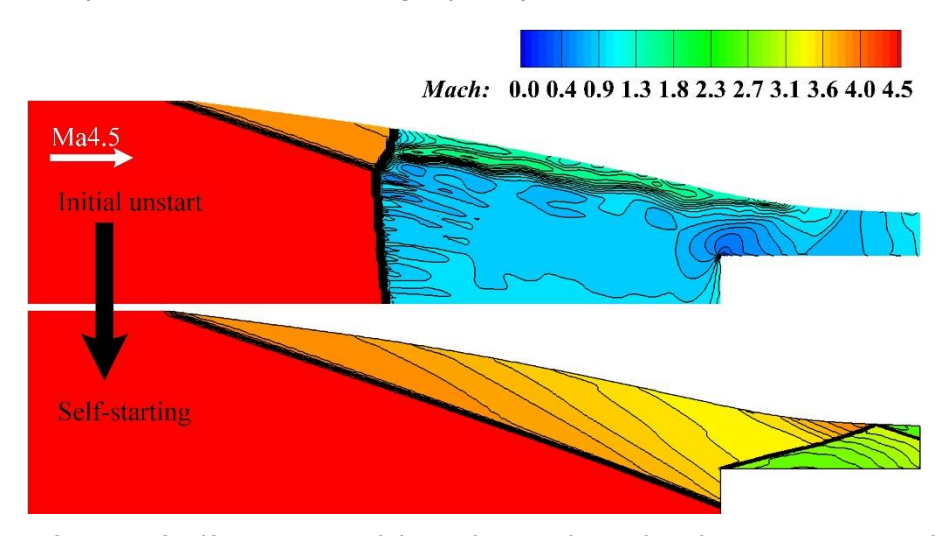


Fig. 10 Verification of self-starting capability at low Mach number design point in DDP basic flow field

# 3.3. Flow characteristics of self-starting inlet

Based on the DDP wide speed range self-starting design method, an inward-turning inlet with a high Mach number design point at Ma6 and a low Mach number design point at Ma4.5 is created. Its high Mach number design point flow characteristics are shown in Fig. 11. The incident shock impinges on the lip leading edge, enabling a shock-on-lip condition and full mass flow capture, with a mass flow rate of 0.99. The reflected shock interacts with the upper wall boundary layer, inducing a shock wave boundary layer interaction (SWBLI), forming a separation bubble on the upper wall.

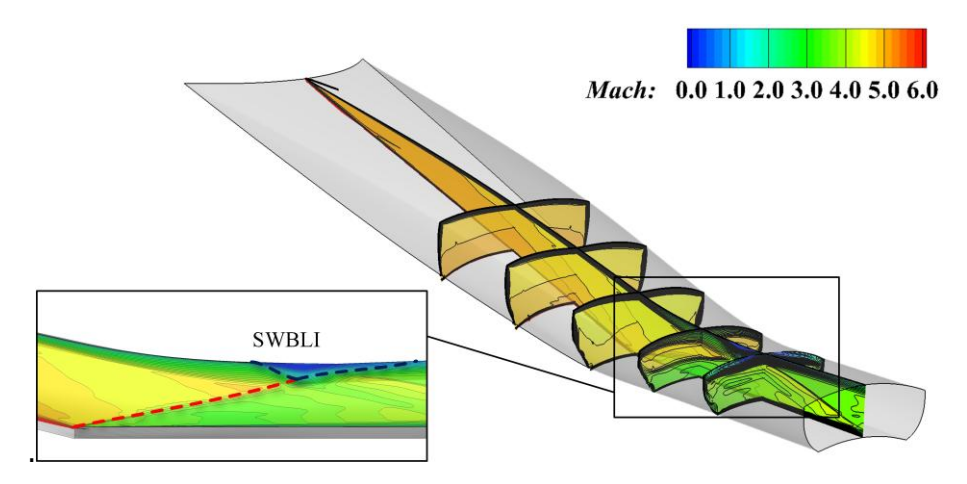


Fig. 11 Flow characteristics of the inlet at high Mach number design point (Ma6)

Fig. 12 illustrates the self-starting process of the inlet. To determine its self-starting critical Mach number, the inflow conditions were incrementally increased. Within the unstarted state at Ma3.8, a large-scale separation dominates the internal contraction section. This separation also induces a separation zone on the lower surface, compromising mass flow capture ability. As Mach number increases, the flow structure changes slightly: both separations diminish in size and migrate towards the throat. By Ma4.4, the lower-surface separation nearly vanishes, while the upper-surface separation propagates downstream of the throat, undergoing significant shape change but remaining large. At Ma4.5, the separation markedly reduces, confirming that self-starting is achieved.

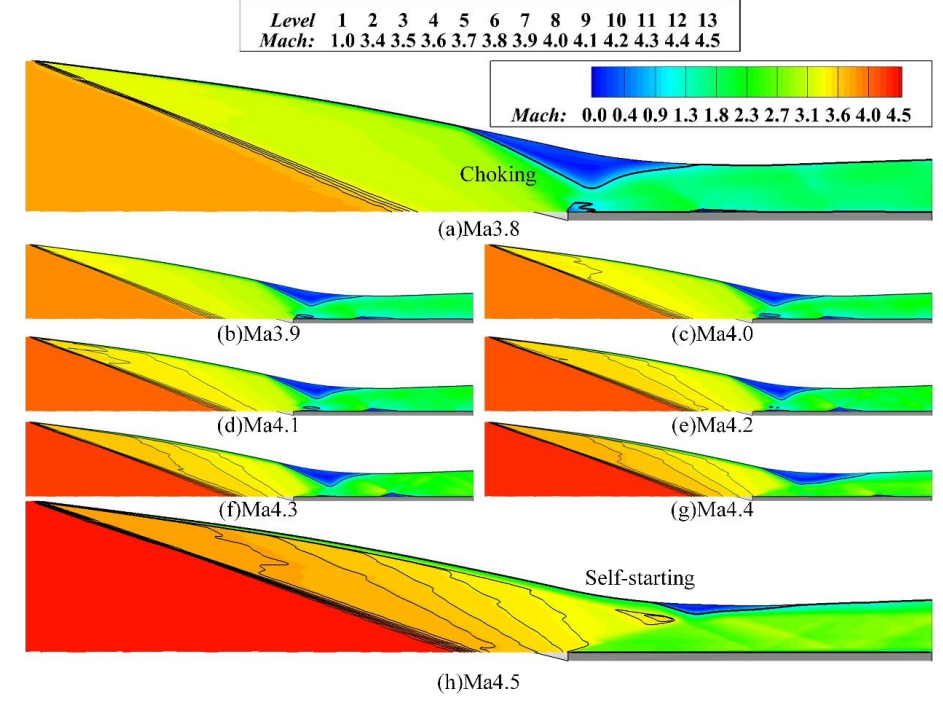


Fig. 12 Self-starting process of osculating inward-turning inlet

## 4. Conculsion

In this study, a double design points method was adopted to construct a basic flow field with widerange self-starting capability for inward-turning inlet design. By controlling the internal contraction section Mach number and contraction ratio at the low Mach number design point, the method enables controlled self-starting capability while ensuring operability across the design range. Validation through numerical simulations confirmed good agreement between the constructed flowfield and computational results. Further self-starting simulations demonstrated that the developed basic flowfield, with design points at Ma6 and Ma4.5, successfully achieved self-starting at Ma4.5, verifying its wide-range operability.

## Reference

- [1] Y. You, An Overview of the Advantages and Concerns of Hypersonic Inward Turning Inlets, in: 17th AIAA International Space Planes and Hypersonic Systems and Technologies Conference, American Institute of Aeronautics and Astronautics, n.d. <a href="https://doi.org/10.2514/6.2011-2269">https://doi.org/10.2514/6.2011-2269</a>. [2]A. Boretti, How close is a hydrogen hypersonic commercial aircraft?, International Journal of Hydrogen Energy 48 (2023) 10684–10691. <a href="https://doi.org/10.1016/j.ijhydene.2022.11.303">https://doi.org/10.1016/j.ijhydene.2022.11.303</a>. [3]S. Walker, M. Tang, C. Mamplata, TBCC Propulsion for a Mach 6 Hypersonic Airplane, in: 16th AIAA/DLR/DGLR International Space Planes and Hypersonic Systems and Technologies Conference, American Institute of Aeronautics and Astronautics, Bremen, Germany, 2009. <a href="https://doi.org/10.2514/6.2009-7238">https://doi.org/10.2514/6.2009-7238</a>.
- [4]J.J. Spravka, T.R. Jorris, Current Hypersonic and Space Vehicle Flight Test Instrumentation Challenges, in: AIAA Flight Testing Conference, American Institute of Aeronautics and Astronautics, Dallas, TX, 2015. https://doi.org/10.2514/6.2015-3224.
- [5]T. Magee, S. Fugal, L. Fink, S. Shaw, Boeing N+2 Supersonic Experimental Validation Phase II Program, in: 32nd AIAA Applied Aerodynamics Conference, American Institute of Aeronautics and Astronautics, Atlanta, GA, 2014. <a href="https://doi.org/10.2514/6.2014-2137">https://doi.org/10.2514/6.2014-2137</a>.
- [6]A. Kantrowitz, Preliminary Investigation of Supersonic Diffusers, (n.d.).
- [7]Wie D M V , D'Alessio S M , White M E .Hypersonic airbreathing propulsion[J].Johns Hopkins Apl Technical Digest, 2005, 26(4):430-436. <a href="https://doi.10.2514/6.1971-662">https://doi.10.2514/6.1971-662</a>.
- [8]D. Van Wie, F. Kwok, R. Walsh, Starting characteristics of supersonic inlets, in: 32nd Joint Propulsion Conference and Exhibit, American Institute of Aeronautics and Astronautics, Lake Buena Vista, FL, U.S.A., 1996. https://doi.org/10.2514/6.1996-2914.
- [9]B. Sun, K. Zhang, Empirical Equation for Self-starting Limit of Supersonic Inlets, Journal of Propulsion and Power 26 (2010) 874–875. https://doi.org/10.2514/1.46798.
- [10]Z. Cai, W. Hu, Z. Hu, C. Shi, X. Zheng, C. Zhu, Y. You, The inverse design and three-dimensional analysis of double design points basic flow field based on wide range capture ability, Aerospace Science and Technology 159 (2025) 109964. https://doi.org/10.1016/j.ast.2025.109964.

HiSST-2025-xxxx Page | 9
Paper Title Copyright © 2025 by author(s)